AD/A-001 086

ANALYSIS OF RAIN EROSION OF COATED AND UNCOATED FIBER REINFORCED COMPOSITE MATERIALS

George S. Springer, et al

Michigan University

Prepared for:

Air Force Materials Laboratory

August 1974

DISTRIBUTED BY:

NTIS

National Technical Information Service
U. S. DEPARTMENT OF COMMERCE

NOTICE

When Government drawings, specifications, or other data are used for any purpose other than in connection with a definitely related Government procurement operation, the United States Government thereby incurs no responsibility nor any obligation whatsoever; and the fact that the Government may have formulated, furnished, or in any way supplied the said drawings, specifications, or other data, is not to be regarded by implication or otherwise as in any manner licensing the holder or any other person or corporation, or conveying any rights or permission to manufacture, use, or sell any patented invention that may in any way be related thereto.

Copies of this report should not be returned unless return is required by security considerations, contractual obligations, or notice on a specified document.

AIR FORCE/56780/21 October 1974 — 300

X

UNCLASSIFIED

SECURITY CLASSIFICATION OF THIS PAGE (When Data Entered)

REPORT DOCUMENTATION PAGE		READ INSTRUCTIONS BEFORE COMPLETING FORM
1 REPORT NUMBER AFML-TR-74-180	2 GOVT ACCESSION NO.	3 RECIPIENT'S CATALOG NUMBER
4 TITLE (and Subtitle) ANALYSIS OF RAIN EROSION OF COATED AND UNCOATED FIBER REINFORCED COMPOSITE MATERIALS		5 TYPE OF REPORT & PERIOD COVERED Technical Report, July 1973-June 1974
		6 PERFORMING ORG. REPORT NUMBER AFML-TR-74-1
7 AUTHOR(s) George S. Springer, Cheng-I. Yang		8 CONTRACT OR GRANT NUMBER(s) F33615-72-C-1563
9 PERFORMING ORGANIZATION NAME AND ADDRESS The University of Michigan, Mechanical Engineering Department, Ann Arbor, Michigan 48104		10 PROGRAM ELEMENT, PROJECT, TASK AREA & WORK UNIT NUMBERS P.E. 62102F, Project 7340 Task 734007, Work Unit 73400755
11 CONTROLLING OFFICE NAME AND ADDRESS Air Force Materials Laboratory, Air Force Systems Command, Wright-Patterson Air Force Base, Ohio 45433		12 REPORT DATE August 1974
		13 NUMBER OF PAGES 48
14 MONITORING AGENCY NAME & ADDRESS(if different from Controlling Office)		15 SECURITY CLASS (of this report) UNCLASSIFIED
		15a DECLASSIFICATION DOWNGRADING SCHEDULE

16 DISTRIBUTION STATEMENT (of this Report)

Approved for public release; distribution unlimited.

17 DISTRIBUTION STATEMENT (of the abstract entered in Block 20, if different from Report)

18 SUPPLEMENTARY NOTES

19 KEY WORDS (Continue on reverse side if necessary and identify by block number)

Rain Erosion
Erosion Mechanism
Fatigue Model
Incubation Period

20 ABSTRACT (Continue on reverse side if necessary and identify by block number)

The behavior of both uncoated and coated fiber reinforced composite substrate systems subjected to repeated impingements of liquid droplets was investigated. The system studied consisted of 1) an uncoated fiber reinforced composite, and 2) a fiber reinforced composite covered by a single layer of homogeneous coating of arbitrary thickness. A macroscopically anisotropic model was developed to approximate the elastic behavior of the fiber reinforced composite. Based on the uniaxial stress wave model, the variations of the stresses with time in the

DD FORM 1 JAN 73 1473 EDITION OF 1 NOV 65 IS OBSOLETE

UNCLASSIFIED

SECURITY CLASSIFICATION OF THIS PAGE (When Data Entered)

i

20.

coat-substrate system were determined both in the coating and in the substrate. Employing the fatigue theorems established for the rain erosion of homogeneous materials, algebraic equations were derived for both systems (1) and (2) which describe the incubation period, rate of mass removal and the total mass loss. The results were compared to available experimental data and good agreement was found between the present analytical results and the data.

FOREWORD

This final report was submitted by Dr. George S. Springer and Dr. Cheng I. Yang of The University of Michigan, Mechanical Engineering Department, Ann Arbor, Michigan, under contract F33615-72-C-1563, Project 7340, Task 734007, with the Air Force Materials Laboratory, Wright-Patterson Air Force Base, Ohio. George F. Schmitt, AFML/MBE was the laboratory project monitor.

This report has been reviewed and cleared for open publication and/or public release by the appropriate Office of Information (OI) in accordance with AFR 190-17 and DODD 5230.9. There is no objection to unlimited distribution of this report to the public at large, or by DDC to the National Technical Information Service (NTIS).

This report covers the period 1 June 1973 to 31 May 1974.

This technical report has been reviewed and is approved for publication.

George F. Schmitt

George F. Schmitt
Project Monitor

Merrill L. Minges, Chief
Elastomers and Coatings Branch

TABLE OF CONTENTS

ILLUSTRATIONS

LIST OF TABLES

NOMENCLATURE

a_1-a_2	constants (dimensionless)
b	constant defined by Eq. (34) (dimensionless)
b_2	knee in the fatigue curve
C	speed of sound (or equivalent wave speed) (ft/sec)
d	diameter of the droplet (ft)
E	Young's modulus (lbf/ft^2)
E_{11}	longitudinal Young's modulus (lbf/ft^2)
E_{22}	transverse Young's modulus (lbf/ft^2)
f	number of stress cycles (Eq. 7)
F	force (lbf)
G	shear modulus (lbf/ft^2)
G_{12}	longitudinal shear modulus (lbf/ft^2)
G_{23}	transverse shear modulus (lbf/ft^2)
h	thickness of coat (ft)
I	rain intensity (ft/sec)
k_e	number of stress wave reflections in the coating required for the stress at coat-substrate interface to reach a value of 63.3 percent of σ_∞ (dimensionless)
k_L	total number of stress wave reflections in the coating (dimensionless)
$\bar{k}$	average number of stress wave reflections in the coating (dimensionless)
m	mass eroded per unit area (lbm/ft^2)
m*	dimensionless mass loss defined by Eq. (56)
n	number of drops impinging per unit area (number/ft^2)
n*	number of drops impinging per site, see Eq.(37)
N	fatigue life, see Eq.(33)(dimensionless)

P	stress (lbf/ft^2)
q	drop density ($number/ft^3$)
r	distance (ft)
S	parameter defined by Eq. (36) (lbf/ft^2)
t	time (sec)
t_L	the duration of impact (sec)
V	velocity of impact (ft/sec)
V_t	terminal velocity of a rain droplet (ft/sec)
V_f	volume fraction of fibers in composite materials (dimensionless)
V_m	volume fraction of matrix in composite materials (dimensionless)
W	weight loss due to erosion (lbf)
Z	dynamic impedance (lbm/ft^2-sec)

Greek Letters

α	rate of mass loss (lbm/impact)
α^*	dimensionless rate of mass loss (see Eq. 52)
ϕ	the angle between axis and fiber's orientation (radians)
ν	Poisson's ratio (dimensionless)
ν_{12}	longitudinal Poisson's ratio (dimensionless)
ν_{21}	transverse Poisson's ratio (dimensionless)
μ_1	$\cos\phi$ (see Eq. 20) (dimensionless)
μ_2	$\sin\phi$ (see Eq. 20) (dimensionless)
ρ	density (lbm/ft^3)
θ	angle of impact (radians)
σ	stress (lbf/ft^2)
$\bar{\sigma}_o$	mean stress at the liquid-coating interface after k_L numbers of stress wave reflections (lbf/ft^2)

σ_I	endurance limit (lbf/ft^2)
σ_u	ultimate tensile strength (lbf/ft^2)
ψ	parameter defined by Eq.(45)

Subscripts

c	coating
f	filament
i	end of incubation period
m	matrix
L	liquid
s	solid
Sc	coat-substrate interface
Lc	liquid-coat interface

SECTION I

INTRODUCTION

Non metallic components constitute an ever increasing portion of modern high speed aircraft, owing to their favorable performance characteristics, including high strength to weight ratio, good magnetic and optical properties etc. Unfortunately, such components are susceptible to heavy damage when subjected to repeated impingements of liquid droplets. In order to utilize the full potential of non metallic components, the damage caused to them by rain erosion must be understood.

The behavior of homogeneous materials (both metallic and non metallic) was investigated extensively experimentally (References 1-9) and analytically (References 3-5, 10-14), and the available results describe well the response of such materials to liquid impingement. However, the rain erosion behavior of fiber reinforced composites has not yet been evaluated fully. Most of the previous studies on reinforced composites are experimental in nature (References 15-20). These studies provide information on the behavior of a given material under a given condition, but fail to describe material behavior beyond the range of the experiments in which they were obtained. Therefore, the objective of this investigation is to develop analytical expressions which are consistent with experimental observations and which predict quantitatively the "erosion" of fiber reinforced materials under previously untested conditions. The model presented here describes a) the "incubation period" i.e. the time elapsed before the mass loss becomes appreciable and b) the mass loss past the incubation period.

The model used in this study is based on fatigue concepts and is designed along the lines developed previously for homogeneous materials (References 13, 14). Here, the model is applied to both coated and uncoated fiber reinforced composites. Study of uncoated composites is important for the general understanding of the rain erosion behavior of such materials. The analysis of coated composites, however, is of greater practical significance, since most uncoated composites have relatively poor resistance to erosion and must be coated for erosion protection.

SECTION II

THE PROBLEM

The problem investigated is the following. Spherical liquid droplets of constant diameter d impinge repeatedly upon a semiinfinite material (Figure 1). Two cases are considered: 1) the material is a fiber reinforced composite composed of unidirectional filaments embedded in a matrix. The material is taken to be semiinfinite normal to the plane of the surface (x direction, Figure 1). 2) The material is a fiber reinforced composite as described in point (1), but is covered by a homogeneous coating of thickness h. In the analysis it is assumed that (a) the composites are macroscopically homogeneous, (b) the fiber filaments are randomly distributed, (c) there is no fiber contiguity, (d) locally both the matrix and the filament are homogeneous and isotropic, (e) the filaments are parallel to the surface, and (f) there is a perfect bond between the matrix and the filaments and, in case of coated composites, between the coating and the substrate (i.e. at the interfaces the stresses and the displacements are continuous). The reinforced composite, the coating, and the droplets are characterized by the properties shown in Figure (1).

The angle of incidence of the droplets θ, and the velocity of impact V are taken to be constant. The spatial distribution of the droplets is considered to be uniform. The number of droplets impinging on unit area in time t may be written as (Reference 13)

$$n = \frac{6}{\pi} \frac{(V\cos\theta)I}{V_t d^3} t \qquad (1)$$

DROPLET

Diameter: d

Density: h_L

Speed of Sound: C_L

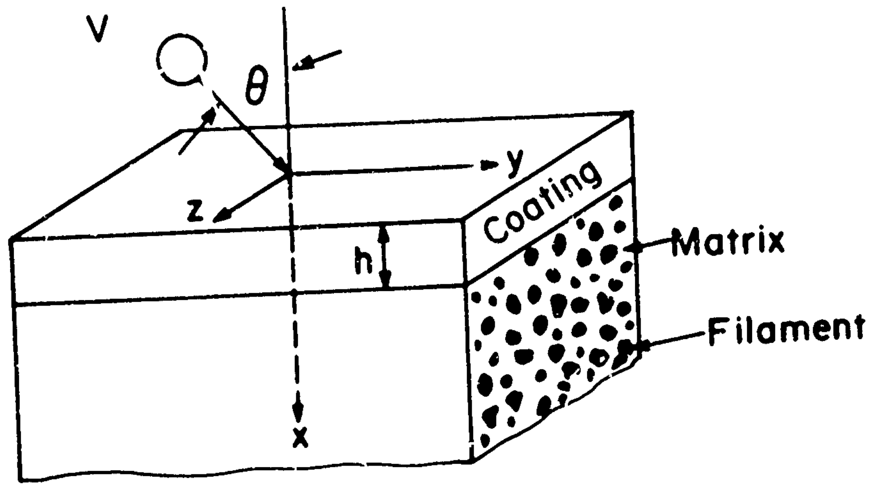

	COATING	SUBSTRATE Matrix	SUBSTRATE Filament
Density	ρ_c	ρ_m	ρ_f
Speed of Sound	C_c	C_m	C_f
Modulus of Elasticity	E_c	E_m	E_f
Poisson Ratio	ν_c	ν_m	ν_f
Ultimate Tensile Strength	$(\sigma_u)_c$	$(\sigma_u)_m$	$(\sigma_u)_f$
Endurance Limit	$(\sigma_I)_c$	$(\sigma_I)_m$	$(\sigma_I)_f$
Volume Fraction		V_m	V_f
Thickness	h		

Figure 1. Droplet Impingement on a Coat-Substrate System

where I is the rain intensity and V_t the terminal velocity of the droplet. The impingement rate is assumed to be sufficiently low so that all the effects produced by the impact of one droplet diminish before the impact of the next droplet (References 4, 13).

The pressure at the liquid-solid interface is taken to be constant and is approximated by the water hammer pressure (Reference 4)

$$P = \frac{\rho_L C_L V \cos\theta}{\frac{\rho_L C_L}{\rho_s C_s} + 1} \tag{2}$$

where ρ and C are the density and the speed of sound. The subscript L and s refer to the liquid and solid, respectively.

For a homogeneous material ρ_s and C_s are the density and speed of sound of the material. For a fiber reinforced composite ρ_s and C_s may be expressed as

$$\rho_s = \rho_f V_f + \rho_m V_m \tag{3}$$

$$C_s = \left[E_{22}/\rho_s\right]^{\frac{1}{2}} \tag{4}$$

where the subscripts f and m refer to the filament and the matrix respectively. V is the volume fraction. E_{22} is the equivalent Young's modulus in the direction normal to the fibers (see equation 16, Section III).

For the purposes of the present analysis equations (2,3,4) represent the pressure with sufficient accuracy. The duration of this pressure is approximated by

$$t_L = \frac{2d}{C_L} \tag{5}$$

The forces, created by the impingements of the droplets, damage the material. This damage manifests itself in different ways, as cracks and pits, and by weight loss of the material. Here, we consider the weight loss to represent material damage, because this parameter was found to describe well the erosion behavior of homogeneous materials (Reference 13). Our model attempts, therefore, to describe the weight loss of the material as a function of time (Figure 2a). However, following the arguments presented in References (13, 14) we replace the total weight loss by mass loss per unit area m, and the time by the number of droplets impinging per unit area n (Figure 2b). The data is then approximated by two straight lines, as shown in Fig. 2b. Accordingly, the mass loss is given by the expressions

$$m = 0 \qquad 0 < n_i \tag{6a}$$

$$m = \alpha(n-n_i) \qquad n_i < n < n_f \tag{6b}$$

In equations (6a, 6b) n_i is the incubation period, a period during which the mass loss is insignificant, α is the rate of mass loss subsequent to the incubation period, and n_f is the limit beyond which the data deviates from the straight line relationship (in most practical situations the usefulness of the material does not extend beyond n_f). Hence, the mass loss- and the erosion damage - can be evaluated, once the parameters n_i, α and n_f are known. Therefore, the problem is to determine these parameters.

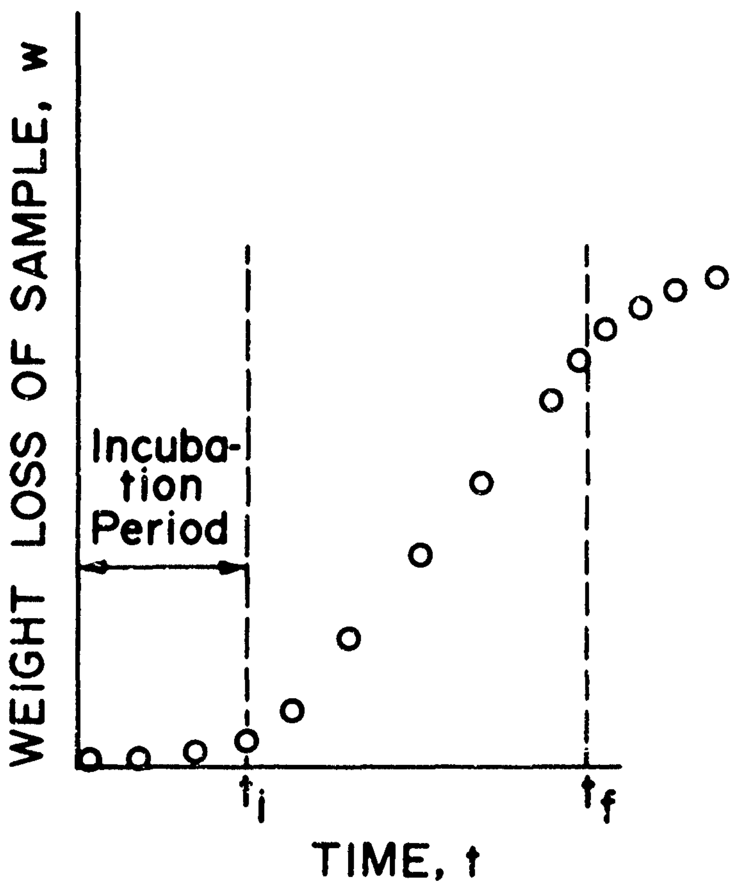

Figure 2a. Schematic of the Experimental Results

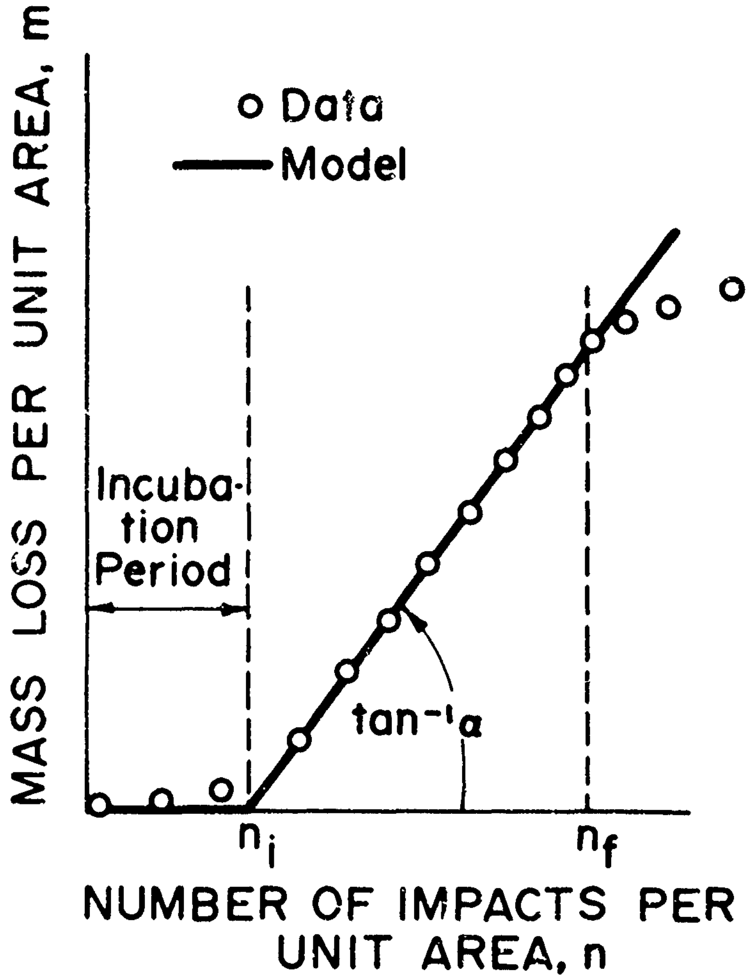

Figure 2b. The Solution Model

SECTION III

INCUBATION PERIOD OF UNCOATED FIBER REINFORCED COMPOSITES

In their previous investigations of coated and uncoated homogeneous materials Springer and his coworkers (References 13, 14) found that the incubation period can be established by applying fatigue theorems to the rain erosion problem. This approach is followed here, and in the following, fatigue concepts are used to determine the incubation period for fiber reinforced composites.

The starting point of the analysis is Miner's rule, which states that the failure of bars undergoing repeated torsion or bending obeys the expression (Reference 21)

$$\frac{f_1}{N_1} + \frac{f_2}{N_2} + \ldots + \frac{f_q}{N_q} = a_1 \tag{7}$$

where f_1, $f_2 \ldots f_q$ represent the number of cycles the specimen is subjected to specified overstress levels σ_1, $\sigma_2 \ldots \sigma_q$, and N_1, $N_2 \ldots N_q$ represent the life (in cycles) at these overstress levels, as given by the fatigue (σ_e versus N) curve. a_1 is a constant .

Let us now consider a point on the surface of the material as shown in Figure 3. Each droplet impinging on the surface creates a stress at point B. This stress may be approximated by

$$\sigma(r,\phi) = \frac{F[1-2\nu(\phi)]}{2\pi\ r^2} \tag{8}$$

Note that σ is a function of both the distance of the point of impact r, and the orientation of the direction of the impact with respect to the direction of the fibers ϕ. The force is taken to be a point force, i.e.

$$F = \frac{\pi d^2}{4} P \qquad (9)$$

where P is the water hammer pressure given by equation (2). ν is the Poisson ratio for the composite in the ϕ direction (see Figure 3) (Reference 24)

$$\nu = E\left[\frac{\nu_{12}}{E_{11}} - \left(\frac{1+2\nu_{12}}{E_{11}} + \frac{1}{E_{22}} - \frac{1}{G_{23}}\right) \mu_1^2\mu_2^2\right] \qquad (10)$$

E is Young's modulus of the composite in the ϕ direction (Reference 24)

$$\frac{1}{E} = \frac{\mu_1^4}{E_{11}} + \left(\frac{1}{G_{23}} - \frac{2\nu_{12}}{E_{11}}\right)\mu_1^2\mu_2^2 + \frac{\mu_2^4}{E_{22}} \qquad (11)$$

and G is the shear modulus of the composite in the ϕ direction (Reference 24)

$$\frac{1}{G} = \frac{1}{G_{12}} + 4\left(\frac{1+2\nu_{12}}{E_{11}} + \frac{1}{E_{22}} - \frac{1}{G_{23}}\right) \mu_1^2\mu_2^2 \qquad (12)$$

In the longitudinal direction (i.e. in the direction parallel to the filaments) the Young's and shear moduli and the Poisson ratio may be written as (References 22, 23, 24).

$$E_{11} = E_f V_f + E_m V_m \qquad (13)$$

$$G_{12} = \frac{(G_f+G_m)\; G_m V_m + 2\; G_f G_m V_f}{(G_f+G_m) V_m + 2\; G_m V_f} \qquad (14)$$

$$\nu_{12} = \nu_f V_f + \nu_m V_m \qquad (15)$$

In the transverse direction (i.e. normal to the filaments) the moduli are

$$E_{22} = \frac{4(\bar{Z}\bar{X}-\bar{Y}^2)G_{23}}{(\bar{X}+G_{23})\bar{Z}-\bar{Y}^2} \tag{16}$$

$$G_{23} = G_m \frac{2V_f G_f (X_m+G_m) + 2V_m G_f G_m + V_m X_m (G_f+G_m)}{2V_f G_m (X_m+G_m) + 2V_m G_f G_m + V_m X_m (G_f+G_m)} \tag{17}$$

$$\nu_{21} = \nu_{12} \frac{E_{22}}{E_{11}} \tag{18}$$

Variables subscripted by f or m refer to properties of the pure filament and the pure matrix, respectively. V_f and V_m are the volume fractions of the filament and the matrix, so that the total volume of the composite is

$$V_s = V_f + V_m = 1 \tag{19}$$

μ_1 and μ_2 are defined as

$$\mu_1 = \cos\phi \tag{20a}$$

$$\mu_2 = \sin\phi \tag{20b}$$

In equation (16) $\bar{X}$, $\bar{Y}$ and $\bar{Z}$ are defined as

$$\bar{X} = \frac{X_m(X_f+G_m)V_m + X_f(X_m+G_m)V_f}{(X_f+G_m)V_m + (X_f+G_m)V_f} \tag{21}$$

$$\bar{Y} = V_f Y_f + V_m Y_m + \left(\frac{Y_f-Y_m}{X_f-X_m}\right)^2 (\bar{X}-V_f X_f-V_m X_m) \tag{22}$$

$$\bar{Z} = 2V_f(1-\nu_f)X_f + 2V_m(1-\nu_m)X_m + \left(\frac{Y_f-Y_m}{X_f-X_m}\right)^2 (\bar{X}-V_f X_f-V_m X_m) \tag{23}$$

where

$$X_{f,m} = \frac{E_{f,m}}{2(1+\nu_{f,m})(1-2\nu_{f,m})} \tag{24}$$

$$Y_{f,m} = \frac{\nu_{f,m}E_{f,m}}{2(1+\nu_{f,m})(1-2\nu_{f,m})} \tag{25}$$

During the incubation period the total number of impacts on an rdrdϕ element located at r is (Figure 3)

$$f(r,\phi) = n_i r\, dr d\phi \tag{26}$$

Accordingly, we write Miner's rule (equation 7) in the form

$$\frac{f(r_1,\phi)}{N_1} + \frac{f(r_2,\phi)}{N_2} + \ldots + \frac{f(r_q,\phi)}{N_q} = a_1 \tag{27}$$

Since r varies continuously from zero to infinity and ϕ from zero to 2π, equation (27) may be written as

$$\int_0^{\infty} \int_0^{2\pi} \frac{n_i r d\phi dr}{N} = a_1 \tag{28}$$

Equation (8) may be rearranged in the form

$$rdr = \frac{1}{2\pi} \frac{F(1-2\nu)}{2\sigma^2} \, d\sigma \tag{29}$$

Substituting equation (29) into equation (28), and using the relationship given by equation (9) we obtain

$$-\int_{\sigma'_u}^{\sigma'_I} \int_0^{2\pi} \frac{n_i \left[\frac{P\pi d^2}{4} \cdot \frac{1}{2\pi} \frac{(1-2\nu)}{2\sigma^2}\right] d\phi d\sigma}{N} \tag{30}$$

The lower and upper limits of the first integral have been changed to the ultimate tensile strength and the endurance limit of the material,

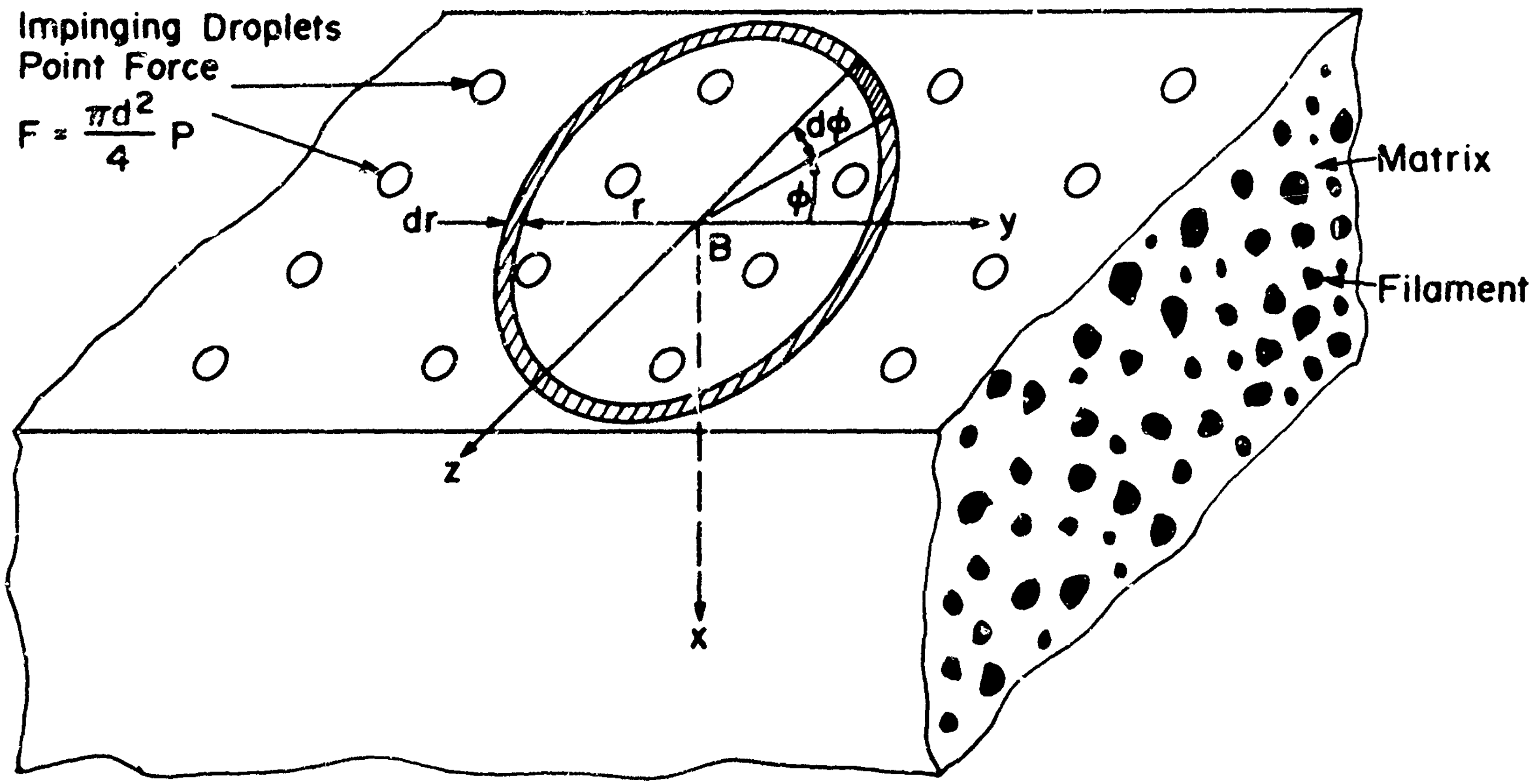

Figure 3. Force Distribution on the Surface

respectively. We shall assume that failure first occurs in the matrix, and approximate σ_u' and σ_I' by

$$\sigma_u' = \sigma_{u_m} \frac{E}{E_m} \tag{31}$$

$$\sigma_I' = \sigma_{I_m} \frac{E}{E_m} \tag{32}$$

where E is given by equation (11). The integrations in equation (30) may be performed once the fatigue life N is known as a function of the stress σ. Following the recommendation presented in References 13, 14, N is expressed as

$$N = \left(\frac{\sigma_u'}{\sigma}\right)^b \tag{33}$$

where

$$b \equiv \frac{b_2}{\log_{10}\left(\frac{\sigma_u'}{\sigma_I'}\right)} \tag{34}$$

b_2 is a constant, such that 10^{b_2} corresponds to the "knee" in the fatigue curve. Substituting equation (33) into equation (30) and integrating we obtain

$$a_1 = \frac{\pi d^2}{4} n_i P \frac{1}{4(b-1)} \frac{E_m}{\sigma_u'} \left[\frac{3}{4}\pi\left(\frac{1}{E_{11}} + \frac{1}{E_{22}}\right) + \frac{\pi}{4}\left(\frac{1}{G_{23}} - \frac{2\nu_{12}}{E_{11}}\right) \right.$$

$$\left. - \frac{4\nu_{12}\pi}{E_{11}} + \left(\frac{1+2\nu_{12}}{E_{11}} + \frac{1}{E_{22}} - \frac{1}{21}\right)\frac{\pi}{4} \right] \tag{35}$$

Introducing the definitions

$$S \equiv \frac{4(b-1)\sigma_u'}{E_m} \left[\frac{3}{4}\pi\left(\frac{1}{E_{11}} + \frac{1}{E_{22}}\right) + \frac{\pi}{4}\left(\frac{1}{G_{23}} - \frac{2\nu_{12}}{E_{11}}\right) - \frac{4\nu_{12}\pi}{E_{11}} \right.$$

$$\left. + \left(\frac{1+2\nu_{12}}{E_{11}} + \frac{1}{E_{22}} - \frac{1}{G_{21}}\right)\frac{\pi}{4} \right]^{-1} \tag{36}$$

$$n_i^* = \frac{\pi d^2}{4} n_i \tag{37}$$

...ation (35) becomes

$$n_i^* = a_1 \frac{S}{P} \tag{38}$$

It is noted now that equation (38) is similar to the expression obtained in reference (13) for homogeneous materials. As in the case of homogeneous materials. S represents the "strength" of the material, while P is the stress produced at the surface. Naturally, the expression for S for reinforced composites (equation 36) is different from the value of S for homogeneous materials (reference 13). However, as one would expect, in the limits a) when there is only one constituent present, i.e. when

$$V_m = 0 \quad V_f = 1 \quad \text{or } V_f = 0 \quad V_m = 1 \tag{39}$$

or b) when the fiber and matrix materials are identical

$$E_m = E_f \quad G_m = G_f \quad \nu_m = \nu_f \quad G_{12} = G_{23} = G_m = G_f \tag{40}$$

equation (36) reduces to the same form as was obtained previously (reference 13) for homogeneous materials.

The foregoing analysis is based on fatigue properties of bars in pure torsion and bending. Consequently, a linear relationship cannot hold between n_i^* and S/P. Therefore, similarly to the procedure used for homogeneous materials we write

$$n_i^* = a_1 \left(\frac{S}{P}\right)^{a_2} \tag{41}$$

where a_1 and a_2 are constants. For homogeneous materials these constants were evaluated by Springer, Yang and Larsen, and were found to be $a_1 = 7.1 \times 10^{-6}$ and $a_2 = 5.7$ (reference 14). The same values of these constants will be used here, i.e.

$$n_i^* = 7.1 \times 10^{-6} \left(\frac{S}{P}\right)^{5.7} \tag{42}$$

The use of the above constants ensures that in the limits given by equations (39) and (40) the foregoing expression yields the result appropriate for a homogeneous material. In other words, equation (42) together with equation (36) may be applied for all volume fractions of the filament from $V_f = 0$ ($V_m = 1$) to $V_f = 1$ ($V_m = 0$). The only limitation on the result is that the incubation period must be greater than zero. The conditions necessary for this limit are further discussed in Section VII.

The validity of the model was evaluated by comparing the above analytical results to experimental data. This comparison, shown in Figure 4 includes all existing data known to us for which the relevant material properties were available. The material properties used in the calculations are listed in Table I.

As can be seen from Figure 4 there is very good agreement between the present result and the data. This lends further confidence to the rain erosion model based on fatigue concepts.

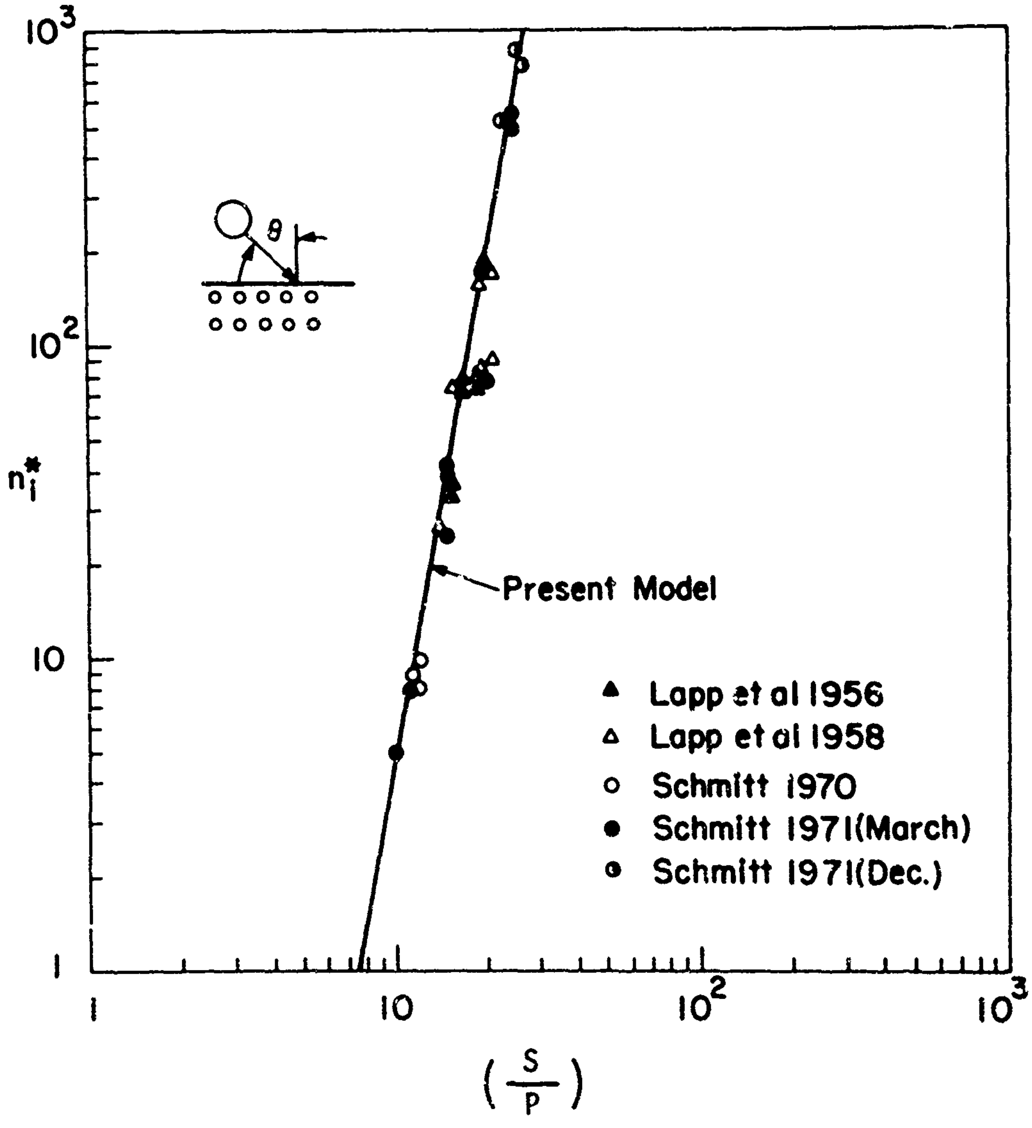

Figure 4. Incubation Period n_i^* versus (S/P). Droplet Impingement on an Uncoated Composite Substrate. Solid Line: Model (Eq. 42) Symbols Defined in Table A-IV

SECTION IV

INCUBATION PERIOD FOR COATED FIBER REINFORCED COMPOSITES

The incubation period for a homogeneous coating on a homogeneous substrate was found by Springer, Yang and Larsen to be (reference 14)

$$n_i^* = 7.1\times10^{-6}\left[\frac{S}{\bar{\sigma}_o}\,\frac{1}{1+\bar{k}\,|\psi_{sc}|}\right]^{5.7} \tag{43}$$

where

$$\bar{k} = k_e\left[1 - \exp\left(-\frac{k_c}{k_e}\right)\right] \tag{44}$$

and

$$\psi_{sc} = \frac{Z_s - Z_c}{Z_s + Z_c}\,; \qquad \psi_{Lc} = \frac{Z_L - Z_c}{Z_L + Z_c} \tag{45}$$

$$k_e = \frac{1 + Z_c/Z_s}{1 + Z_L/Z_s} \tag{46a}$$

$$k_L = \frac{C_c}{C_L}\,\frac{d}{h} \tag{46b}$$

$$\bar{\sigma}_o = P\,\frac{1+\psi_{sc}}{1-\psi_{sc}\psi_{Lc}}\left[1 - \psi_{sc}\,\frac{1+\psi_{Lc}}{1+\psi_{sc}}\,\frac{1-\exp\left(-\frac{k_L}{k_e}\right)}{\left(\frac{k_L}{k_e}\right)}\right] \tag{47}$$

and Z is the impedance of the material

$$Z = \rho C \tag{48}$$

Note that in the absence of the coating the incubation period is

$$n_i^* = 7.1\times10^{-6}\left(\frac{S}{P}\right)^{5.7} \tag{49}$$

where P denotes the impact stress at the surface. Thus, the factor $[1 + \bar{k}\,|\psi_{sc}|\,]^{-1}$ represents the damping effect of the coating.

It is noted, however, that the results, given by equations (43-49). are valid even when the substrate is a fiber reinforced composite material, provided the fibers are randomly distributed and the composite can be taken to be quasihomogeneous. In this case the impedance of the substrate can be approximated by $Z_s = \rho_s C_s$ where

$$C_s = [E_s/\rho_s]^{\frac{1}{2}} = \left[\frac{E_{22}}{\rho_f V_f + \rho_m V_m}\right]^{\frac{1}{2}} \qquad (50)$$

The incubation period can thus be calcu'-ted from equation (43), together with equation (36). The calculated values of the incubation period are compared to available experimental data in Figure 5. The material properties used in the calculations are listed in Table I. Again good agreement is evident between the calculated results and the data.

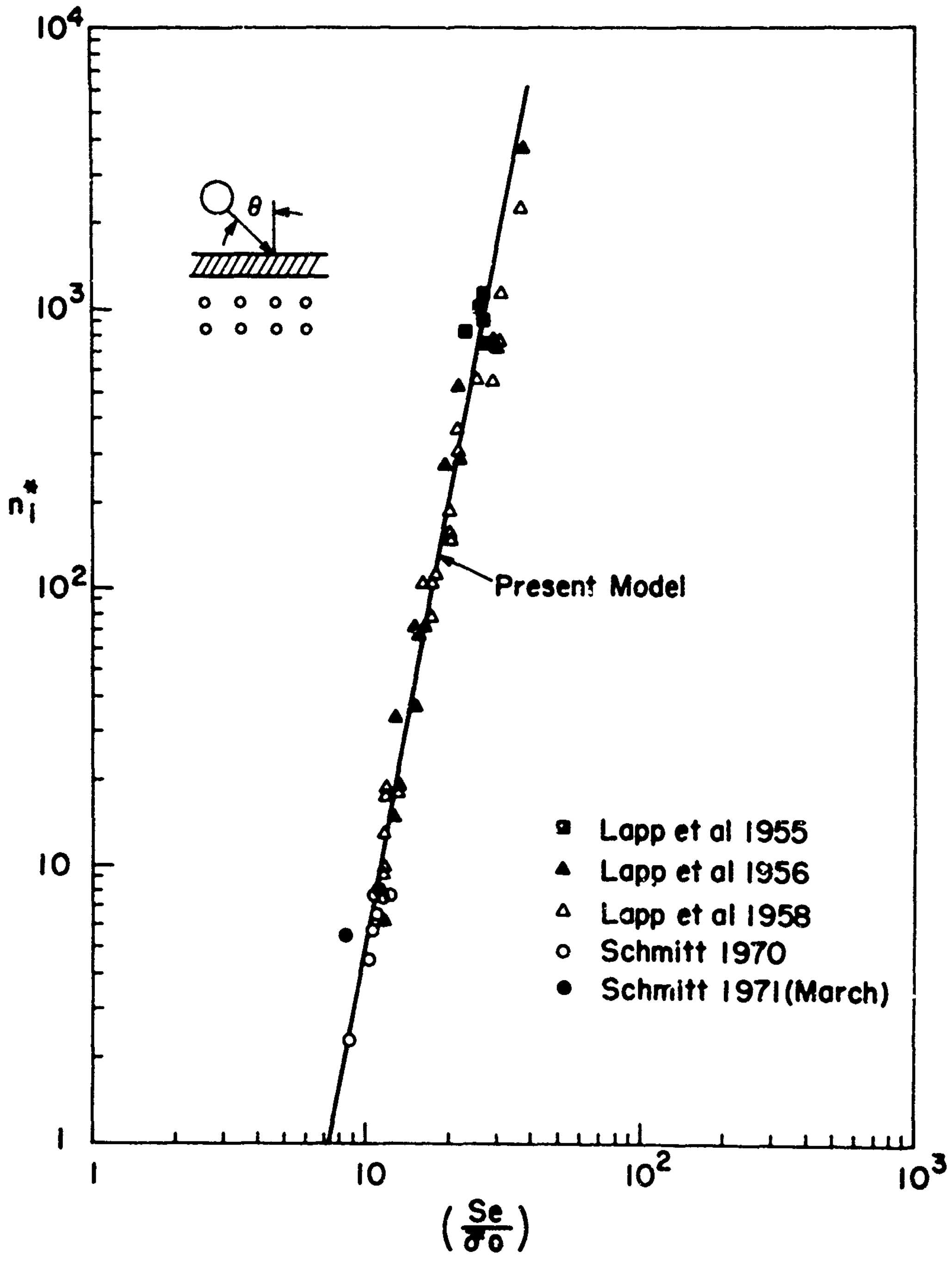

Figure 5. Incubation Period n_i^* versus $(S_e/\bar{\sigma}_o)$. Droplet Impingement on a Coated Composite Substrate. Solid Line: Model (Eq. 43). Symbols Defined in Table A-V

SECTION V

RATE OF MASS REMOVAL

The rate of mass removal for a homogeneous material was calculated by Springer and Baxi (13) and for a homogeneous material covered by a homogeneous coating by Springer, Yang and Larsen (14). For both of these cases the mass removal rate was found to be

$$\alpha^* = 0.023 \left(\frac{1}{n_i^*}\right)^{0.7} \qquad (51)$$

where α^* is defined as

$$\alpha^* = \frac{\alpha}{\pi \rho d^3/4} \qquad (52)$$

The agruments leading to the above results could be repeated, without any modification, for fiber reinforced composite materials. Since the analyses for homogeneous materials are presented in detail in references (13, 14) they will not be reproduced here. It suffices to say that the above result is applicable to fiber reinforced composite materials (both with and without coating) as well as to homogeneous materials. Naturally, the appropriate equation must be used in evaluating n_i^*. For a fiber reinforced composite material n_i^* must be calculated from equation (42). For a fiber reinforced composite material covered with a single layer of homogeneous coating, n_i^* is to be determined from equation (43).

In equation (52) ρ is the density of the material undergoing erosion. Thus, for an uncoated fiber reinforced composite material ρ is given by equation (3). In the case of a coated material ρ is the density of the coating.

The rates of mass removal, calculated from equation (51) together with equation (42) (for uncoated reinforced composite) and equation (43) (for coated composites) are shown in Figures 6 and 7. In these figures the available experimental data are also given. The agreement is again good between the analytical results obtained from the present model, and the data.

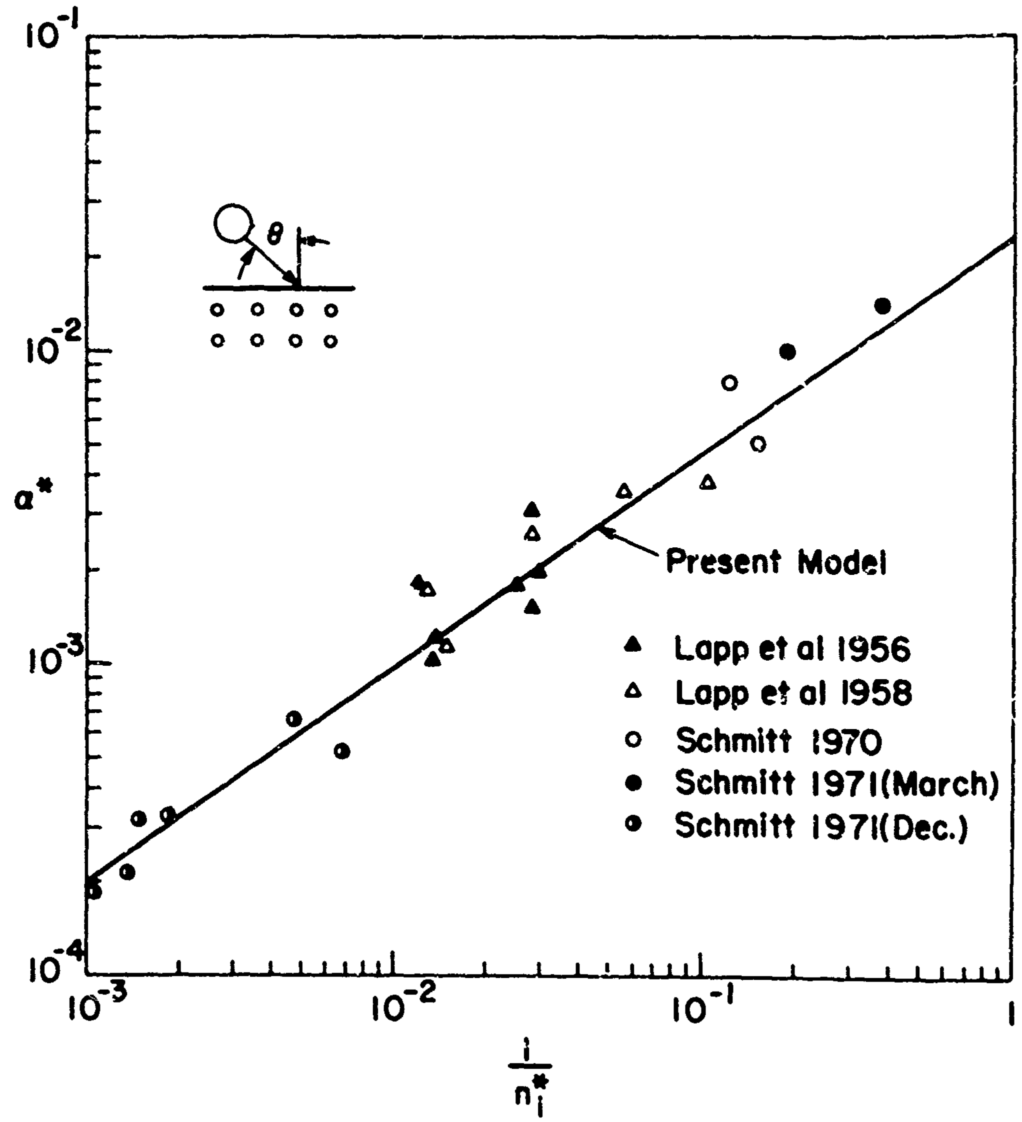

Figure 6. Rate of Erosion versus the Inverse of the Incubation Period. Droplet Impingement on an Uncoated Composite Substrate. Solid Line: Model (Eq. 51). Symbols Defined in Table A-IV

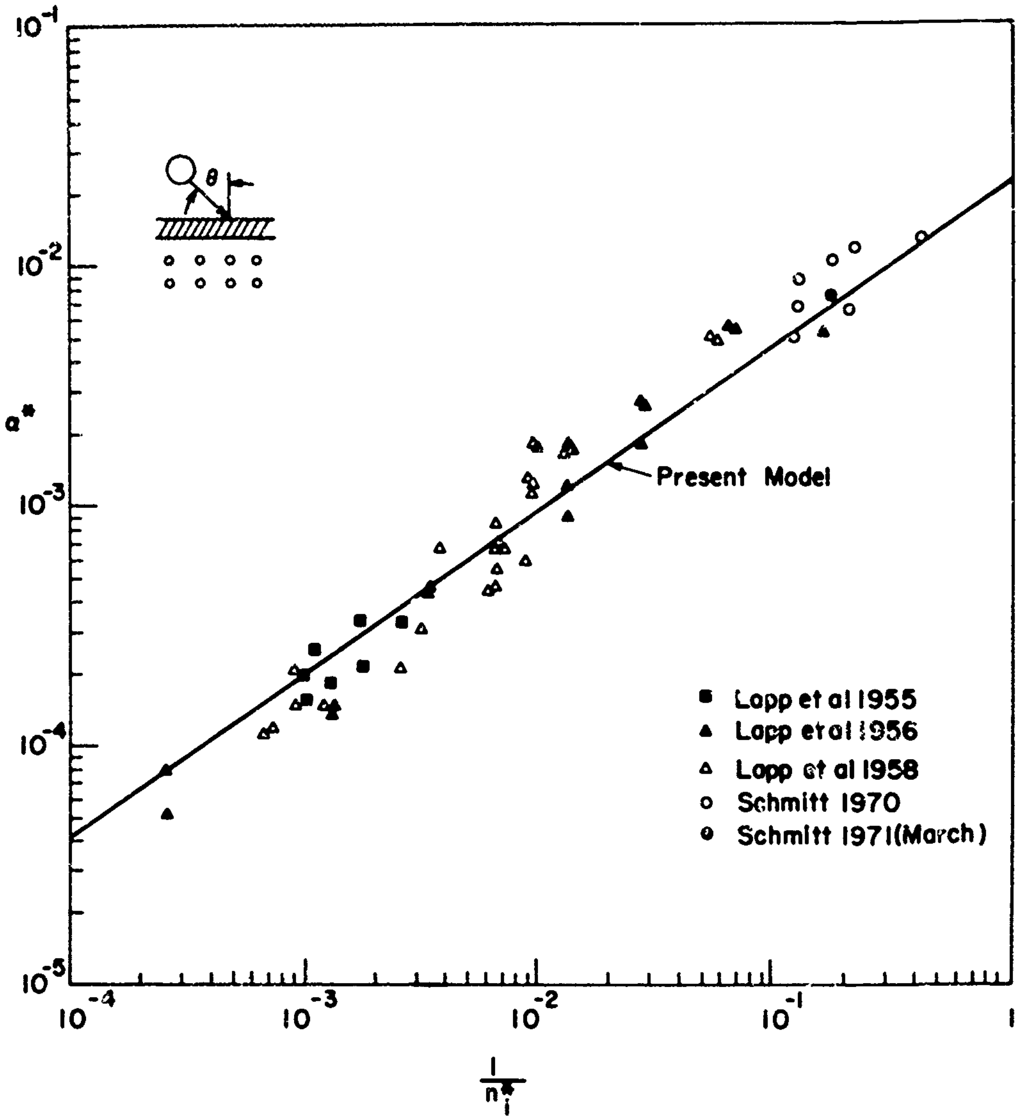

Figure 7. Rate of Erosion versus the Inverse of the Incubation Period. Droplet Impingement on a Coated Composite Substrate. Solid Line: Model (Eq. 51). Symbols Defined in Table A-V

SECTION VI

TOTAL MASS LOSS

The total mass loss was given by equation (6b) as

$$m = \alpha(n-n_i) \tag{53}$$

This equation is rewritten now in dimensionless form

$$m^* = \alpha^* \; (n^*-n_i^*) \tag{54}$$

or

$$\frac{m^*}{\alpha^*} = n^*-n_i^* \tag{55}$$

Here the dimensionless mass loss rate is defined as

$$m^* = \frac{m}{\rho d} \tag{56}$$

When there is no coating present ρ is the density of the composite as given by equation (3). When the reinforced composite is coated by a homogeneous material ρ is the density of the coating.

Equation (55) is valid for both coated or uncoated materials. In calculating the mass loss rate from this equation, the correct forms of n_i^* must be used. For an uncoated fiber reinforced composite material n_i^* is given by equation (42). For a fiber reinforced composite covered by a homogeneous coating n_i^* is given by equation (43).

Using equation (55) all the available data can be correlated on a m^*/α^* versus $n^*-n_i^*$ plot. Such correlations are presented on Figures 8 and 9. In Figure 8 the analytical results are compared to the data for the case of uncoated composites. In Figure 9 a similar comparison is given for coated composites. The material properties used in obtaining these figures are listed in Table I. The agreement between the data and the theoretical line is very good, in fact remarkable in view of the unavoidable errors inherent in many of the measurements. It must be emphasized, that the theoretical lines in Figures 8 and 9 are direct results of the calculations, and are in no way "matched" to the data shown in these figures.

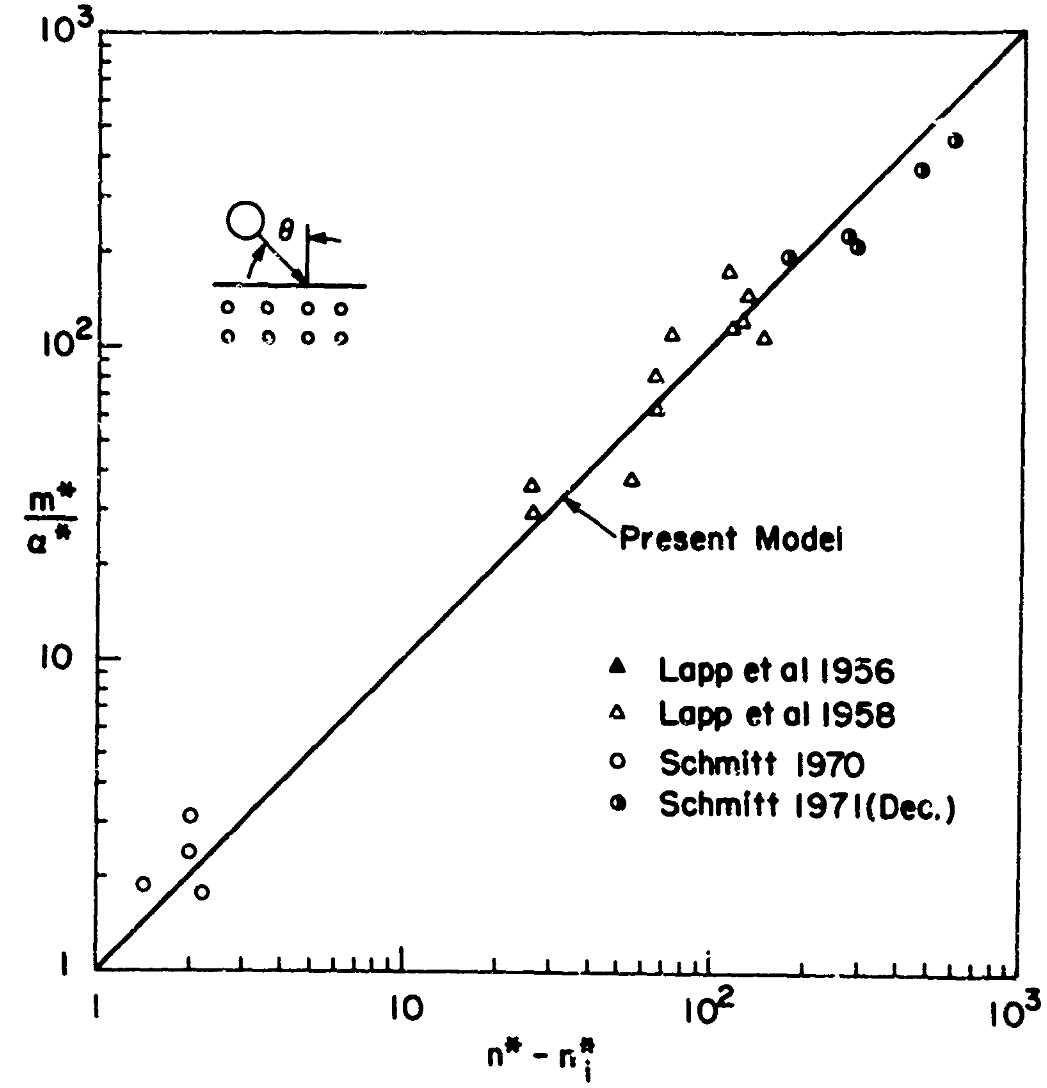

Figure 8. Comparison of Present Model (Solid Line: Eq. 55) with Experimental Results. Droplet Impingement on an Uncoated Composite Substrate. Symbols Defined in Table A-IV

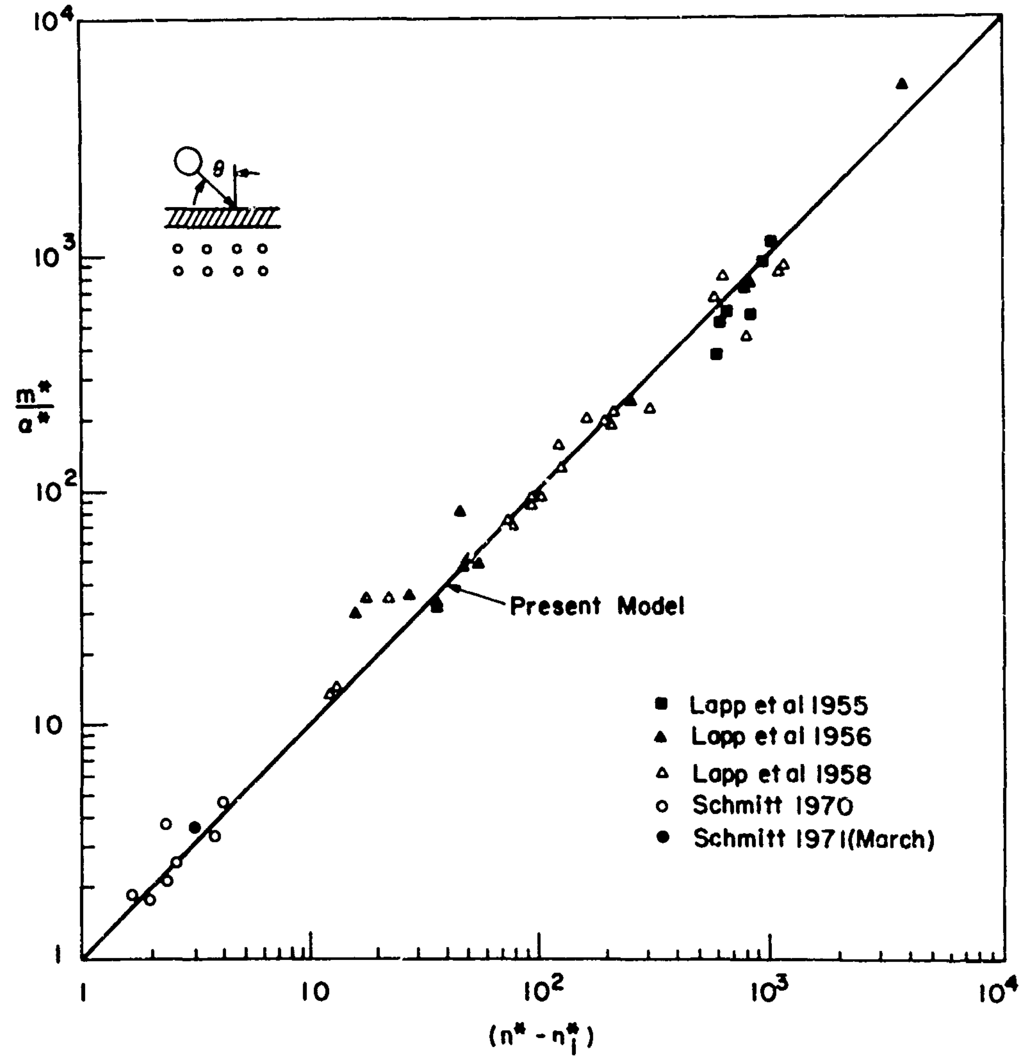

Figure 9. Comparison of Present Model (Solid Line: Eq. 55) with Experimental Results. Droplet Impingement on a Coated Composite Substrate. Symbols Defined in Table A-V

SECTION VII

LIMITS OF APPLICABILITY OF MODEL

The results presented in the foregoing sections are valid when the following two conditions are satisfied: (1) there is a finite incubation period and (2) the mass loss varies linearly with the number of impacts n (i.e. with time t). The first of these conditions is met when the following inequality is satisfied

$$n_i^* > 1 \tag{57}$$

For a fiber reinforced composite without coating this condition may also be expressed as (see equation 42)

$$\frac{S}{P} > 8 \tag{58}$$

For a fiber reinforced composite covered with a homogeneous coating a finite incubation period exists if (see equation 43)

$$\frac{S}{P} \frac{1}{1 + \bar{k} \quad |\psi_{cs}|} > 8 \tag{59}$$

Equations (57, 58, 59) provide the lower limit of the applicability of the model. The upper limit beyond which the present model cannot be applied is determined by the second condition given above. This limit was estimated by observing that up to about $n = 3n_i$ the data do not deviate significantly from the model. This condition may be expressed as

$$n < 3n_i \tag{60}$$

For an uncoated fiber reinforced composite this condition is satisfied when

$$n^* < 3n_i^* \tag{61}$$

For coated composites the upper limit of the applicability of the model is given by the combination of equations (2,49) and (59). The result is

$$n^* < 3n_i^* \tag{62}$$

It must be emphasized that conditions (57) and (60) are the only constraints imposed on the model. No further restrictions are placed on either the material or the impact velocity.

SECTION VIII

SUMMARY

In the following tables a summary of the equations is presented. The following tables are included in this summary

Table I. Definition of Parameters

Table II. Equations Describing Rain Erosion of Fiber Reinforced Composite Materials

Table III. Equations Describing Rain Erosion of Fiber Reinforced Composite Materials Covered with a Homogeneous Coating.

Table I. Definition of Parameters

Density of Composite Material	ρ_s	$\rho_m V_m + \rho_f V_f$
Elastic Constants in the ϕ Direction (see Figure 3) Note: $\mu_1 = \cos\phi$ $\mu_2 = \sin\phi$	E	$\left[\frac{\mu_1^4}{E_{11}} + \left(\frac{1}{G_{23}} - \frac{2\nu_{12}}{E_{11}}\right)\mu_1^2\mu_2^2 + \frac{\mu_2^4}{E_{22}}\right]^{-1}$
	G	$\left[\frac{1}{G_{12}} + 4\left(\frac{1 + 2\nu_{12}}{E_{11}} + \frac{1}{E_{22}} - \frac{1}{G_{23}}\right)\mu_1^2\mu_2^2\right]^{-1}$
	ν_{12}	$\nu_f V_f + \nu_m V_m$
	ν_{21}	$\nu_{12} \frac{E_{22}}{E_{11}}$
	ν	$E\left[\frac{\nu_{12}}{E_{11}} - \left(\frac{1 + 2\nu_{12}}{E_{11}} + \frac{1}{E_{22}} - \frac{1}{G_{23}}\right)\mu_1^2\mu_2^2\right]$
Equivalent Wave Speed in Transverse Direction of Composite	C_s	$[E_{22}/\rho_s]^{1/2}$
Equivalent Dynamic Impedance in Transverse Direction of Composite	Z_s	$\rho_s C_s$

Table I (continued)

Dynamic Impedance of the Liquid Droplet (diameter d)	Z_L	$\rho_L C_L$
Dynamic Impedance of Coating (thickness h)	Z_c	$\rho_c C_c$
Number of Stress Wave Reflections in the Coating after Impact by Droplet (reference 14)	$\bar{k}$	$\frac{1}{1 - \psi_{Sc}\psi_{Lc}} [1 - \exp(- \frac{k_L}{k_c})]$
	ψ_{Sc}	$\frac{Z_s - Z_c}{Z_s + Z_c}$
	ψ_{Lc}	$\frac{Z_L - Z_c}{Z_L + Z_c}$
	k_L	$\frac{C_0}{C_L} \frac{d}{h}$
	k_e	$\frac{1 + Z_c/Z_s}{1 + Z_L/Z_s}$

Table II. Equations Describing Rain Erosion of Fiber Reinforced Composite Materials

Strength Parameter S	$\frac{4\sigma_u(b-1)}{E_m}\left[\frac{3\pi}{4}\left(\frac{1}{E_{11}}+\frac{1}{E_{22}}\right)+\frac{\pi}{4}\left(\frac{1}{G_{23}}-\frac{2\nu_{12}}{E_{11}}\right)-\frac{4\nu_{12}\pi}{E_{11}}+\frac{\pi}{4}\left(\frac{1+2\nu_{12}}{E_{11}}+\frac{1}{E_{22}}-\frac{1}{G_{21}}\right)\right]^{-1}$	lbf/ft^2
Stress Parameter P (lbf/ft^2)	$\frac{Z_L V\cos\theta}{1+Z_L/Z_S}$	lbf/ft^2
Incubation Period n_i^*	$7.1\times10^{-6}\left[\frac{S}{P}\right]^{5.7}$	dimensionless
n_i	$\frac{9.05\times10^{-6}}{d^2}\left[\frac{S}{P}\right]^{5.7}$	$\frac{\text{number of impacts}}{\text{unit area}}$
t_i	$\frac{9.05\times10^{-6}}{qV\cos\theta d^2}\left[\frac{S}{P}\right]^{5.7}$	seconds

Table II (continued)

Rate of Mass Removal α^*	$92 \left[\frac{P}{S}\right]^4$	dimensionless
α	$70.6\rho_s d^3 \left[\frac{P}{S}\right]^4$	$\frac{\text{mass loss}}{\text{impact}}$
Total Mass Loss m^*	$\alpha^* (n^* - n_i^*)$	dimensionless
m	$70.6\rho_s d^3 \left[\frac{P}{S}\right] \quad (qtV\cos\theta) - \frac{9.05\times10^{-6}}{d^2} \left(\frac{S}{P}\right)^{5.7}$	$\frac{\text{mass loss}}{\text{unit area}}$

Table III. Equations Describing Rain Erosion of Fiber Reinforced Composite Covered with a Homogeneous Coating

Strength Parameter S_e	$\frac{4\sigma_u(b-1)}{(1-2\nu_c)[1 + 2\bar{k}\lvert\psi_{sc}\rvert]}$	lbf/ft^2
Stress Parameter $\bar{\sigma}_o$	$\frac{Z_L V \cos\theta}{1 + Z_L/Z_c} \frac{1 + \psi_{Sc}}{1 - \psi_{Sc}\psi_{Lc}} [1 - \psi_{SC} \frac{1 + \psi_{Lc}}{1 + \psi_{Sc}} \frac{1 - \exp(\frac{k_L}{k_e})}{(\frac{k_L}{k_e})}]$	lbf/ft^2
Incubation Period n_i^*	$7.1\times10^{-6} [\frac{S_e}{\bar{\sigma}_o}]^{5.7}$	dimensionless
n_i	$\frac{9.05\times10^{-6}}{d^2} (\frac{S_e}{\bar{\sigma}_o})^{5.7}$	$\frac{\text{number of impact}}{\text{unit area}}$
t_i	$\frac{9.05\times10^{-6}}{qV\cos\theta d^2} (\frac{S_e}{\bar{\sigma}_o})^{5.7}$	seconds

Table III (continued)

Rate of Mass Removal α^*	$92\left(\frac{\bar{\sigma}_o}{S_e}\right)^4$	dimensionless
α	$70.6\rho_c d^3 \left(\frac{\bar{\sigma}_o}{S_e}\right)^4$	$\frac{\text{mass loss}}{\text{impact}}$
Total Mass Loss m^*	$\alpha^* (n^* - n_i^*)$	dimensionless
m	$70.6\rho_c d^3 \left(\frac{\bar{\sigma}_o}{S_e}\right) (qtV\cos\theta) - \frac{9.05\times10^{-6}}{d^2} \left(\frac{S_e}{\sigma_o}\right)^{5.7}$	$\frac{\text{mass loss}}{\text{unit area}}$

APPENDIX

In this appendix, the following tables are included

Table A-I. Material Properties Used in the Calculations for Fiber Reinforced Composites

Table A-II. Material Properties Used in the Calculations for Coating Materials

Table A-III. Dynamic Properties of Composite Materials

Table A-IV. Description of Data and Symbols Used in Figures 4,6,8

Table A-V. Description of Data and Symbols Used in Figure 5,7,9

Table A-I. Material Properties Used in the Calculations for the Reinforced Composites* (b=20.9)

	Fiber Content %	E_{11} lb/in^2 x 10^6	E_{22} lb/in^2 x 10^6	G_{12} lb/in^2 x 10^6	G_{23} lb/in^2 x 10^6	ν_{12}	matrix x10^3 σ_u lb/in^2	ρ g/c.c.
glass-polyester	65	5.3	1.2	0.55	0.24	0.25	6.5	1.85
glass-epoxy	65	6.7	2.5	1.0	0.30	0.25	8.4	1.84
boron-epoxy	65	30.0	3.0	1.0	0.8	0.22	8.4	2.19
graphite-epoxy	65	25.3	1.2	0.65	0.2	0.31	8.4	1.47
glass-polyimide	65	7.9	2.9	1.0	0.3	0.25	8.0	1.98
ceramic-teflon	65	2.88	0.95	0.5	0.2	0.25	2.0	1.85
glass-polyphenylene	65	2.59	0.85	0.5	0.2	0.25	2.0	1.82
glass-silicone	65	10.0	3.6	1.0	0.8	0.3	9.0	2.2

* From reference 25

Table A-11. Material Properties Used in the Calculations for Coating Materials** (b=20.9)

	Density ρ $\frac{lb\text{-}sec^2}{in^4}$ $\times 10^{-4}$	Wave speed C $\frac{in}{sec}$ $\times 10^4$	Dynamic Impedance $Z = \rho C$ $lb\text{-}sec/in^3$	σ_u lb/in^2 $\times 10^3$	ν
water	0.94	5.76	5.35		
polyurethane	0.93	1.08	1.00	2.0	0.2
neoprene	1.45	0.53	0.78	1.2	0.2
alumina	3.56	21.9	78.4	1.7	0.25
Polyethylene	0.89	5.80	5.16	1.4	0.2
nickel	7.87	19.65	15.4	2.6	0.3
silicon	2.07	22.5	46.6	7.16	0.16
teflon (hypalon)	2.12	2.11	4.48	3.2	0.3

** From reference 26

Table A-III. Dynamic Properties of Composite Materials

Composite Material	Equivalent Density ρ $lb\text{-}sec^2/in^4 \times 10^{-4}$	Equivalent Wave Speed $C = \sqrt{E_{22}/\rho}$ $in/sec \times 10^4$	Equivalent Dynamic Impedance $Z = \rho C$ $lb\text{-}sec/in^3$
glass-polyester	1.97	7.82	15.4
glass-epoxy	1.95	8.95	17.1
boron-epoxy	2.34	13.1	30.6
graphite-epoxy	1.56	8.5	12.7
glass-polyimide	1.86	12.4	23.10
ceramic-teflon	1.74	7.39	12.85
glass-polyphenylene	1.71	7.05	12.05
glass-silicone	2.07	13.18	27.28

Table A-IV. Description of Data and Symbols Used in Figures 4, 6, 8

Symbol	Investigators	Materials: Fiber	Materials: Matrix	Impact Velocity ft/sec	Rain Intensity (in/hr)	Drop Size mm	% Fiber
▲	Lapp et al 1956 (ref. 16)	glass	polyester	731	1	1.9	65
			epoxy				
△	Lapp et al 1958 (ref. 17)	glass	polyester	731	1	1.9	65
			epoxy				
			polyimide				
		ceramic	teflon				
○	Schmitt & Krabill 1970 (ref. 19)	glass	epoxy	1596	2.5	1.9	69
			silicone	2360			
			polyester	2751			
			polyphenylene	4246			
		boron	epoxy				55-65
		graphite					

Table A-IV (continued)

Symbol	Investigators	Materials		Impact Velocity ft/sec	Rain Intensity (in/hr)	Drop Size mm	% Fiber
		Fiber	Matrix				
●	Schmitt 1971 (ref. 20)	boron	epoxy	731	1	1.8	55-65
		graphite					
◑	Schmitt 1971 (ref. 27)	glass	polyimide	731	1	1.8	65
			epoxy				
		graphite	epoxy				55-65
		boron					

Table A-V. Description of Data and Symbols Used in Figures 5, 7, 9

Symbol	Investigator	Coating	Substrate Fiber	Substrate Matrix	Coating Thickness mils	Impact Velocity ft/sec	Rain Intensity in/hr	Drop Size mm	% Fiber
■	Lapp et al 1955 (ref. 15)	silicon	glass	polyester	10	731	1	1.9	65
		neoprene			1,4,5,7,8, 9,10.13,14, 21.22,27-33				
▲	Lapp et al 1956 (ref. 16)	neoprene	glass	polyester	4-5, 10	731	1	1.9	65
		polyurethane			2,4,5,11,23				
		polyethylene			7				
		neoprene	glass	epoxy	10				
		teflon			2,5				
△	Lapp et al 1958 (ref. 17)	neoprene	glass	polyester	5,6,8,10-15	731	1	1.9	65
		polyurethane			20, 5-10				
		polyurethane	glass	epoxy	10,14,15-20, 20-25, 25-30				

Table A-V (continued)

Symbol	Investigator	Coating	Substrate Fiber	Substrate Matrix	Coating Thickness mils	Velocity ft/sec	Intensity in/hr	Drop Size mm	% Fiber
○	Schmitt & Krabill 1970 (ref. 19)	nickel	glass	epoxy	12,15	3169 4291 2216 2280	2.5	1.9	69
◕	Schmitt 1971 (ref. 20)	polyurethane	boron	epoxy	8,12	731	1	1.8	55-65
		nickel							
		polyurethane	graphite	epoxy					
		nickel							
		urethane	boron	epoxv	10	1593,23 2360	2.5	1.9	55-65
		nickel							

Table A-V (continued)

Symbol	Investigator	Coating	Substrate		Coating Thickness mils	Impact Velocity ft/sec	Rain Intensity in/hr	Drop Size mm	% Fiber
			Fiber	Matrix					
△	Lapp et al 1958 (ref. 17)	teflon	glass	epoxy	10, 15	731	1	1.9	65
		hypalon	glass	epoxy	9				
○	Schmitt & Krabill 1970 (ref. 19)	alumina	glass	epoxy	20,30,40	1593 2246 2426	2.5	1.9	69
			glass	polyimide	30				
		neoprene	glass	epoxy	10	1556 2220			
		urethane			5,10,15,20 30	1556 2220 2350			
		polyethylene			30	1678 2216 2451			
		urethane	boron	epoxy	10	1593 2360			55-65

REFERENCES

[1] Eisenberg, P., "Cavitation and Impact Erosion-Concepts, Correlations, Controversies," Characterization and Determination of Erosion Resistance, ASTM STP 474, American Society for Testing and Materials, pp. 3-28, 1970.

[2] Engel, O., "Mechanism of Rain Erosion-A Critical Review of Erosion by Water Drop Impact," WADC Technical Report 53-192, Part 6, Wright-Patterson Air Force Base, Dayton, Ohio, July 1955.

[3] Heymann, F.J., "A Survey of Clues to the Relation Between Erosion Rate and Impingement Conditions," Proceedings of the Second Meersburg Conference on Rain Erosion and Allied Phenomena (edited by A.A. Fyall and R.B. King), Royal Aircraft Establishment, Farnborough, England, pp. 359-388, August 1967.

[4] Heymann, F.J., "Erosion by Cavitation, Liquid Impingement and Solid Impingement: A Review," Engineering Report E-1460, Westinghouse Electric Corporation, Lester, Pennsylvania, March 1968.

[5] Heymann, F. and Arcella, F.,"Analytical Investigation of Turbine Erosion Phenomenon," WANL-PR-(DD)-014, Westinghouse Astronuclear Laboratory, Westinghouse Electric Corporation, Lester, Pennsylvania, November 1966.

[6] Wahl, N.E., "Investigation of the Phenomena of Rain Erosion at Subsonic and Supersonic Speeds," AFML-TR-65-330, Air Force Materials Laboratory, Wright-Patterson Air Force Base, Dayton, Ohio, October 1965.

[7] Fyall, A.A. and King,R.B.,editors, "Proceedings of the Rain Erosion Conference," held at Meersburg, West Germany, May 1965, translated proceedings available from: Royal Aircraft Establishment, Farnborough, England.

[8] Fyall, A.A. and King,R.B.,editors, "Proceedings of the Second Meersburg Conference on Rain Erosion and Allied Phenomena," August 1967, translated Proceedings available from: Royal Aircraft Establishment, Farnborough, England.

[9] Fyall, A.A.,editor, "Proceedings of the Third Conference on Rain Erosion and Allied Phenomena," Royal Aircraft Establishment, Farnborough, England, August 1970.

[10] Hammitt, F.G., Huang, Y.C., Kling, C.L., Mitchell, T.M., Jr., Solomon, L.P., "A Statistically Vertical Model for Correlating Volume Loss Due to Cavitation or Liquid Impingement," in Characterization and Determination of Erosion Resistance, ASTM STP 474, American Society for Testing and Materials, pp. 288-322, 1970.

[11] Morris, J.W., Jr. and Wahl, N.E., "Supersonic Rain and Sand Erosion Research: Erosion Characteristics of Aerospace Materials," AFML-TR-70-265, Air Force Materials Laboratory, Wright-Patterson Air Force Base, Dayton, Ohio, November 1970.

[12] Schmitt, G.F., Jr., Tatnall, G.J. and Foulke, K.W., "Joint Air Force-Navy Supersonic Rain Erosion Evaluations of Materials," AFML-TR-67-164, Air Force Materials Laboratory, Wright-Patterson Air Force Base, Dayton, Ohio, December 1967.

[13] Springer, G.S., Baxi, C.B., "A Model for Rain Erosion of Homogeneous Material," Technical Report AFML-TR-72-106, Air Force Materials Laboratory, Wright-Patterson Air Force Base, Dayton, Ohio, June 1972.

[14] Springer, G.S., Yang, C.I., and Larsen, P.S., "Analysis of Rain Erosion of Coated Materials," Technical Report AFML-TR-73-227, Air Force Materials Laboratory, Wright-Patterson Air Force Base, Dayton, Ohio, September 1973.

[15] Lapp, R.R., Stutzman, R.H. and Wahl, N.E., "A Study of the Rain Erosion of Plastic and Metals," WADC Technical Report 53-185, part 2. Wright-Patterson Air Force Base, Dayton, Ohio, May 1955.

[16] Lapp, R.R., Stutzman, R.H., and Wahl, N.E., "Summary Report on the Rain Erosion of Aircraft Materials at High Speed in Rain," WADC Technical Report 53-185, Part 3. Wright-Patterson Air Force Base, Dayton, Ohio, September 1956.

[17] Lapp, R.R., Thorpe, D.H., Stutzman, R.H., and Wahl, N.E., "The Study of Erosion of Aircraft Materials at High Speed in Rain," WADC Technical Report 53-185, part 4. Wright-Patterson Air Force Base, Dayton, Ohio, May 1958.

[18] Schmitt, G.F., "Research for Improved Subsonic and Supersonic Rain Erosion Resistant Materials," AFML-TR-67-211, Air Force Materials Laboratory, Wright-Patterson Air Force Base, Dayton, Ohio, January 1968.

[19] Schmitt, G.F., Krabill, A.H., "Velocity-Erosion Rate Relationships of Materials in Rain at Supersonic Speeds," AFML-TR-70-44, Air Force Materials Laboratory, Wright-Patterson Air Force Base, Dayton, Ohio, October 1970.

[20] Schmitt, G.F., "Materials Parameters that Govern the Rain Erosion Behavior of Polymeric Coatings and Composites at Subsonic Velocities," Technical Report AFML-TR-71-197, Air Force Materials Laboratory, Wright-Patterson Air Force Base, Dayton, Ohio, December 1971.

[21] Miner, M.A., "Cumulative Damage in Fatigue," Journal of Applied Mechanics, Vol. 12, pp. A159-A164, 1945.

[22] Hermans, J.J., "The Elastic Properties of Fiber-Reinforced Materials when the Fibers are Aligned," Koninkelijke Nederlandse Akademic Van Wetenschappen, Amsterdam, Proceedings, Series B, Vol. 70, No. 1 (1967), pp. 1-11.

[23] Hill, R., "Theory of Mechanical Properties of Fiber-Strengthened Materials, I. Elastic Behavior," Journal of the Mechanics and Physics of Solids, Vol. 12 1964 , pp. 199-218.

[24] Zecca, A.R., and Hay, D.R., "Elastic Properties of Metal-Matrix Composites," Journal of Composite Materials, Vol. 4, 1970 , pp. 556-561.

[25] Kicher, T.P., "The Analysis of Unbalanced Cross-Piled Elliptic Plates Under Uniform Pressure," Journal of Composite Materials, Vol. 3, 1969 , pp. 424-432.

[26] Conn, A.F., and Rudy, S.L., "Further Research on Predicting the Rain Erosion Resistance of Materials," The Technical Report 7107-1, Hydronautics, Laurel, Maryland, May 1972.

[27] Schmitt, G.F., Jr., "Rain-Erosion of Graphite and Boron-Fiber-Reinforced Epoxy Composite Material," Technical Report AFML-TR-70-316, Air Force Materials Laboratory, Wright-Patterson Air Force Base, Dayton, Ohio, March 1971.

☆U.S. Government Printing Office: 1974 — 657-014/134